Kinetics of turbulent hetero-coagulation of oppositely charged colloidal particles

著者	SUGIMOTO Takuya, WATANABE Yuji, KOBAYASHI Motoyoshi
journal or publication title	Theoretical and applied mechanics Japan
volume	63
page range	133-145
year	2015
URL	http://hdl.handle.net/2241/00124903

doi: 10.11345/nctam.63.133

Kinetics of turbulent hetero-coagulation of oppositely charged colloidal particles

Takuya SUGIMOTO* · Yuji WATANABE** · Motoyoshi KOBAYASHI***

*Graduate School of Life and Environmental Sciences, University of Tsukuba, Tsukuba
**Former Faculty of Agriculture, Iwate University, Iwate
***Faculty of Life and Environmental Sciences, University of Tsukuba, Tsukuba

We investigated the hetero-coagulation rates between oppositely charged particles subjected to a turbulent flow. The turbulent hetero-coagulation was induced by mixing and stirring the aqueous suspensions of positively and negatively charged latex particles. The sign and magnitude of the surface charge densities of the particles were confirmed by the analysis of measured electrophoretic mobilities. The turbulent coagulation experiments were carried out as a function of particle diameter, KCl concentration, and turbulent intensity. The rate of coagulation was obtained by measuring temporal change of suspension turbidity. The experimental results show that the hetero-coagulation rate constant increases with decreasing KCl concentration and with increasing particle size and turbulent intensity. These trends qualitatively agree with the theoretical prediction based on the aggregation kinetics in a turbulent flow combined with a trajectory analysis including the attractive electrostatic interactions. The facilitated coagulation rates in lower KCl concentrations are considered to be due to the increase of the magnitude of attractive electrostatic force accompanied by the development of electrical double layer.

1. INTRODUCTION

Understanding coagulation of colloidal particles is important to control the flow property of solid-liquid multiphase fluid, to advance the aggregation process in water treatment, and also to predict the colloid facilitated transport in water environments.[1),2)] The coagulation kinetics is controlled by the collision rate between particles. Theoretical collision rates induced by Brownian motion and a simple shear flow were formulated by Smoluchowski.[3)] The theoretical rate in an isotropic turbulence was derived by Saffman and Turner.[4)] Unfortunately, these expressions overestimate the experimental rate of coagulation because of neglecting the hydrodynamic interaction as well as physico-chemical interactions. The latter interaction forces considered usually are mainly composed of the van der Waals force and electrical double layer force and are called the Derjaguin-Landau-Verwey-Overbeek (DLVO) force.[10),11)] To take account of these inter-particle interactions, capture efficiency, which is the ratio of actual coagulation rate to the theoretical rate neglecting any interactions, is generally introduced as a correction factor.[5)–8)]

The capture efficiency for Brownian coagulation can be calculated by using the modified Fuchs formula,[6),9)] which is derived by calculating the inward-particle flux to a reference particle due to the Brownian diffusion and the DLVO force[10),11)] with hydrodynamic retardation effect. Experimental

verification of the theory for Brownian coagulation[12),13)] demonstrated that the theory underestimates the coagulation rate in the presence of the electrical double layer repulsion. However, recently, Behrens *et al.*[14)] showed that the theoretical rate for Brownian coagulation quantitatively agrees with the experimental coagulation rate even in the presence of the double layer repulsion in the case of low surface charge density and low electrolyte concentration.

The capture efficiency in a simple shear flow has been evaluated by using a trajectory analysis that describes particle colliding trajectories under the influences of hydrodynamic interaction and the DLVO force.[7),8),15)–21)] Although the trajectory analysis is strictly valid in a simple shear flow, the trajectory analysis is applied to the turbulent coagulation as a first approximation. This is because the flow in the smallest eddy of a turbulence may be expected to be analogous to the shear flow with a mean local shear rate in the turbulence.[22)] The validity of this approximation has been confirmed by previous researchers.[22)–27)]

A lot of previous studies on coagulation kinetics focused on the homo-coagulation between equal sized and similarly charged particles in aqueous suspensions. In the mixture of positively and negatively charged particles, the hetero-coagulation between oppositely charged particles occurs. Although the hetero-coagulation process is important from engineering and scientific point of view, the limited number of studies have been performed on the kinetics of hetero-coagulation. The study of Brownian hetero-coagulation rates between oppositely charged particles demonstrated that the hetero-coagulation rate increases with decreasing electrolyte concentration and that the rate weakly depends on the magnitude of surface potential.[28)] Similar conclusions were obtained for the deposition rate of colloidal particles onto oppositely charged collectors.[29)] Their experimental values of stability ratios, which are the reciprocals of coagulation rates normalized by the rate in the absence of double layer force, are in quantitative agreement with the theory including the DLVO force. While the similar behavior reported in the literature[28)] is expected to be observed for shear-induced coagulation such as in a simple shear flow and turbulence, experiments of turbulent coagulation between oppositely charged particles have never been systematically conducted in authors' knowledge. Due to the lack of experimental data, in spite of the existence of the calculation based on the trajectory analysis with attractive double layer force,[20)] the validity of the theory has not yet been examined by the comparison between experimental and theoretical values.

In the present study, we measured the hetero-coagulation rate between oppositely charged and equal sized particles in a turbulent flow for the first time. The turbulent hetero-coagulation was induced by stirring the mixture of positively charged amidine latex particles and negatively charged sulfate latex particles in aqueous solution. Absolute hetero-coagulation rates were determined from the temporal change of absorbance due to the formation of aggregates by using the T-matrix method.[30)] The obtained values are analyzed by the trajectory analysis with the DLVO force including attractive double layer force.

2. THEORY

Turbulent coagulation rate constant β_{SA} can be expressed by multiplying the capture efficiency $\alpha_{T,SA}$[22)] to the rate constant neglecting any interparticle interaction derived by Saffman and Turner;[4)]

$$\beta_{SA} = \alpha_{T,SA}(2R)^3\sqrt{\frac{8\pi\epsilon_T}{15\nu}} \tag{1}$$

where R the particle radius, ν the kinematic viscosity of the medium and ϵ_T the rate of energy dissipation per unit mass in a turbulent flow, respectively. Eq. (1) assumes that colliding particles have the same radius. This assumption was satisfied in all of our experiments.

We calculate the capture efficiency $\alpha_{T,SA}$ based on trajectory analysis with the DLVO the-

ory.[7),8),21)] The schematic representation of the trajectory analysis is shown in Fig. 1. The trajectory analysis is strictly valid in a simple shear flow. However, we apply the trajectory analysis to the turbulent coagulation as a first approximation because the flow in the smallest eddies of a turbulence is expected to be analogous to the shear flow with a mean local shear rate in the turbulence.[22)] This assumption is presumable if the length scale where coagulation occurs is smaller than the Kolmogoroff microscale of the turbulence. The validity of this approximation has been confirmed by previous researchers.[22)–27)]

Let us consider two colliding particles with a radius of R and with two different surface charge densities of σ_i $(i = 1,\ 2)$ which satisfy a inequality, $|\sigma_1| > |\sigma_2|$, in a simple shear flow with a mean shear rate of $G_T = \sqrt{4\epsilon_T/(15\pi\nu)}$. The relative position of the two particles can be expressed in the Cartesian (x, y, z) or the spherical (r, θ, ϕ) coordinates. The temporal evolution of the relative position obeys the relative particle velocity given by the following trajectory equations.[16)]

$$\frac{dr^*}{dt^*} = r^*(1 - \mathcal{A}(r^*, \rho)) \sin^2\theta \sin\phi \cos\phi + \frac{\mathcal{C}(r^*, \rho)}{6\pi\eta G_T R^2}(F_{vdW} + F_{edl}) \tag{2}$$

$$\frac{d\theta}{dt^*} = (1 - \mathcal{B}(r^*, \rho)) \sin\theta \cos\theta \sin\phi \cos\phi \tag{3}$$

$$\frac{d\phi}{dt^*} = \cos^2\phi - \frac{\mathcal{B}(r^*, \rho)}{2} \cos 2\phi \tag{4}$$

where t time, $r^* = r/R$ dimensionless center-to-center distance of the particles, $t^* = G_T t$ dimensionless time, ρ size ratio, and η the viscosity of the medium, respectively. $\mathcal{A}$, $\mathcal{B}$, $\mathcal{C}$ are also hydrodynamic interaction functions depending on ρ and r^*.

The far-field expressions for $\mathcal{A}$, $\mathcal{B}$, $\mathcal{C}$ are described as[6),31)]

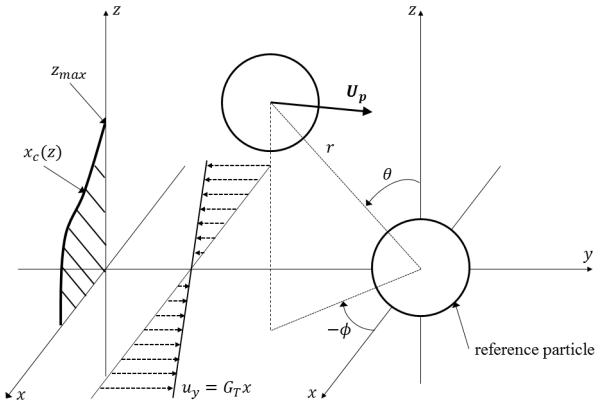

Fig. 1 Schematic representation of a trajectory analysis. $\boldsymbol{U_p}$ the particle relative velocity described by Eqs. (2-4), $x_c(z)$ the boundary between aggregation or not on $x - z$ plane at the released point$(y = -100R)$, and z_{max} the maximum of z on the boundary, respectively.

$$\mathcal{A}(r^*,\rho) = \frac{5(1+\rho^3)}{2r^{*3}} - \frac{3(1+\rho^5)+5\rho^2(1+\rho)}{2r^{*5}} + \frac{25\rho^3}{r^{*6}} \tag{5}$$

$$\mathcal{B}(r^*,\rho) = \frac{1+\rho^5+(5/3)\rho^2(1+\rho)}{r^{*5}} \tag{6}$$

$$\mathcal{C}(r^*,\rho) = 1+\frac{1}{\rho} \tag{7}$$

On the one hand, the near-field expressions for those are shown as[16)]

$$\mathcal{A}(r^*,\rho) = 1-4.077h^* \tag{8}$$

$$\mathcal{B}(r^*,\rho) = 0.4060+\frac{0.78}{\ln h^*} \tag{9}$$

$$\mathcal{C}(r^*,\rho) = 4h^*(1+1.34h^*\ln h^*) \tag{10}$$

where $h^* = r^* - \rho - 1$ is the dimensionless surface separation distance. In the intermediate distance, the interpolated expressions listed by Wang[17)] are adopted in this calculation. In this study, we use the expressions of $\mathcal{A}$, $\mathcal{B}$, $\mathcal{C}$ for $\rho = 1$ given by previous researchers,[6),15)–17),31)] because the colliding particles have the same radius R in our experiments.

In Eq. (2), F_{vdW} and F_{edl} are the van der Waals attractive force and the electrical double layer force, respectively. The van der Waals attraction taking account of the retardation effect is calculated using the following expressions;[18)–20)] that is, if $p < 0.590$,

$$F_{vdW} = -\frac{A_{\mathrm{H}}R}{2h^2}\frac{1+3.54p}{6(1+1.77p)^2} \tag{11}$$

and if $p \geq 0.590$,

$$F_{vdW} = -\frac{A_{\mathrm{H}}R}{2h^2}\left(\frac{2.45}{15p}-\frac{2.17}{30p^2}+\frac{1.18}{105p^3}\right) \tag{12}$$

where $h = r - 2R$ surface separation distance between two equal size particles, A_{H} the Hamaker constant, and $p = 2\pi h/\lambda_{\mathrm{L}}$ dimensionless distance in which λ_{L} is the London wavelength and has been mainly taken $\lambda_{\mathrm{L}} = 100$ nm. The value of λ_{L} is comparable to the travel distance of light during one rotation of a Bohr atom electron[35)] because the intramolecular charge distribution affects the induced dipole moment which is the origin of the van der Waals attraction.

In symmetrical ($z:z$ type) electrolyte solutions such as KCl, F_{edl} can be calculated by using the Derjaguin approximation which estimates the sphere-sphere interaction as the sum of plate-plate interaction as follows:[32)–34)]

$$F_{edl} = \pi R\int_h^\infty P(L)dL \tag{13}$$

where $P(L)$ are the electrical double layer force per unit area between two plates with a plate-to-plate distance of L. In this study, the $P(L)$ is calculated using the Ohshima equation for electrical double layer force.[32),34)] If the electrolyte is symmetrical, $P(L)$ can be related to an integration constant C which emerges as a result of integrating the Poisson-Boltzmann equation as[34)]

$$P(L) = -\frac{n_0}{\beta}(C+2) \tag{14}$$

where n_0, and $\beta = 1/(k_B T)$ are the bulk concentration of the electrolyte, and the inverse thermal energy. k_B, and T are Boltzmann constant, and absolute temperature, respectively. When the surface charge densities σ_i of both surfaces are constant irrespective of the surface separation and have opposite sign with unequal magnitude, we can determine the plate-to-plate distance L in terms of the given $P(L)$ through the C (i.e. Eq. (14)). For $C = -2$ (corresponds to zero double layer force), $L = L_0$ is given by

$$\kappa L_0 = \ln\left[\frac{|\sigma_1'|(2+\sqrt{\sigma_2'^2+4})}{|\sigma_2'|(2+\sqrt{\sigma_1'^2+4})}\right] \tag{15}$$

where $\kappa = \sqrt{2\beta n_0 e^2/(\epsilon_r\epsilon_0)}$ the Debye parameter, e the elementary charge, $\epsilon_r\epsilon_0$ the permittivity of the medium, respectively, $\sigma_1' = \beta e\sigma_1/(\epsilon_r\epsilon_0\kappa)$ and $\sigma_2' = \beta e\sigma_2/(\epsilon_r\epsilon_0\kappa)$ where the σ_1 is larger surface charge density in magnitude than that of σ_2. In the region of $L < L_0$ corresponding to $C < -2$ (repulsive force region), L is expressed by

$$\kappa L = \frac{2}{\sqrt{-C+2}}\left[F\left\{\frac{2}{\sqrt{-C+2}}\middle|\arctan\left(\frac{|\sigma_1'|}{\sqrt{-C-2}}\right)\right\} - F\left\{\frac{2}{\sqrt{-C+2}}\middle|\arctan\left(\frac{|\sigma_2'|}{\sqrt{-C-2}}\right)\right\}\right] \tag{16}$$

where $F(m|\phi)$ is an elliptic integral of the first kind defined by

$$F(m|\phi) = \int_0^{\phi}\frac{d\phi'}{\sqrt{1-m^2\sin^2\phi'}} \tag{17}$$

In the region of $L > L_0$ corresponding to $C > -2$ (attractive force region), the electrical double layer force has the minimum value P_m at the $L = L_m$ given by

$$P(L_m) = P_m = -\frac{n_0}{\beta}\sigma_2'^2 \tag{18}$$

$$\kappa L_m = \begin{cases} F\left[\sqrt{1-\left(\frac{\sigma_2'}{2}\right)^2}\middle|\arccos\left|\frac{\sigma_2'}{\sigma_1'}\right|\right] & \text{for } |\sigma_2'| \le 2 \\ \frac{2}{|\sigma_2'|}\left[K\left\{\sqrt{1-\left(\frac{2}{\sigma_2'}\right)^2}\right\} - F\left\{\sqrt{1-\left(\frac{2}{\sigma_2'}\right)^2}\middle|\arcsin\left|\frac{\sigma_2'}{\sigma_1'}\right|\right\}\right] & \text{for } |\sigma_2'| \ge 2 \end{cases} \tag{19}$$

where $K(m)$ is a complete elliptic integral of the first kind defined by $K(m) = F(m|\pi/2)$. Eq. (18) means that the minimum value of (in other words, maximum attractive) double layer force is proportional to the square of smaller surface charge density in magnitude σ_2^2 irrespective of larger magnitude of surface charge density σ_1. In the region $L_0 < L < L_m$, L is given by

$$\kappa L = \begin{cases} F\left\{\frac{1}{2}\sqrt{-C+2}\middle|\arccos\left(\frac{\sqrt{C+2}}{|\sigma_1'|}\right)\right\} - F\left\{\frac{1}{2}\sqrt{-C+2}\middle|\arccos\left(\frac{\sqrt{C+2}}{|\sigma_2'|}\right)\right\} & \text{for } -2 < C \le 2 \\ \frac{2}{\sqrt{C+2}}\left[F\left\{\sqrt{\frac{C-2}{C+2}}\middle|\arcsin\left(\frac{\sqrt{C+2}}{|\sigma_2'|}\right)\right\} - F\left\{\sqrt{\frac{C-2}{C+2}}\middle|\arcsin\left(\frac{\sqrt{C+2}}{|\sigma_1'|}\right)\right\}\right] & \text{for } C \ge 2 \end{cases} \tag{20}$$

On the other hand, in the region $L > L_m$, L is given by

$$\kappa L = \begin{cases} F\left\{\frac{1}{2}\sqrt{-C+2}\middle|\arccos\left(\frac{\sqrt{C+2}}{|\sigma_1'|}\right)\right\} + F\left\{\frac{1}{2}\sqrt{-C+2}\middle|\arccos\left(\frac{\sqrt{C+2}}{|\sigma_2'|}\right)\right\} & \text{for } -2 < C \leq 2 \\ \frac{2}{\sqrt{C+2}}\left[2K\left(\sqrt{\frac{C-2}{C+2}}\right) - F\left\{\sqrt{\frac{C-2}{C+2}}\middle|\arcsin\left(\frac{\sqrt{C+2}}{|\sigma_2'|}\right)\right\} - F\left\{\sqrt{\frac{C-2}{C+2}}\middle|\arcsin\left(\frac{\sqrt{C+2}}{|\sigma_1'|}\right)\right\}\right] & \text{for } C \geq 2 \end{cases} \tag{21}$$

The temporal evolution of relative position of two colliding particles can be calculated by using Eqs. (2)-(4) by the forth Runge-Kutta method. In this calculation, we systematically change released points of a particle from $x - z$ plane at $y^* = y/R = -100$ in the velocity field $u_y = G_T x$ as represented in Fig. 1. Each trajectory of the released particle from a release point results in a fate in a deterministic way; aggregation occurs or not. The calculation was continued until the relative position of the particles resulted in one of the following three cases as (i) $r^* - 2 < \epsilon^* = \epsilon/R$, where ϵ is the minimum separation, (ii) $\phi > \pi/2$, or (iii) $y^* = 10$. The former two cases (i) and (ii) correspond to aggregation. The last case (iii) indicates that each particle is separated and no aggregation occurs. In this study, $\epsilon^* = 10^{-7}$ was adopted to avoid computational divergence.[18] The boundary between aggregation or not on $x - z$ plane at the released point, $x_c(z)$, and the maximum of z on the boundary, z_{max} can be evaluated with the trajectory analysis. The $x_c(z)$ and the z_{max} characterize the capture cross section which expresses the released point that aggregation occurs as the shaded area shown in Fig. 1. Since evaluating the $x_c(z)$ and z_{max} is equivalent to estimate the particle inflow flux into the reference particle, the capture efficiency $\alpha_{T,SA}$ is calculated as follows[7),8),13),18)–20)]

$$\alpha_{T,SA} = \frac{3}{16}\int_0^{z^*_{max}} [x_c^*(z^*)]^2 dz^* \tag{22}$$

where $z^* = z/R$, z^*_{max} and $x_c^*(z^*) = x_c/R$.

3. EXPERIMENTS

3.1. Materials

We used four different types of monodisperse polystyrene latex particles which were in the aqueous stock suspensions purchased from Interfacial Dynamics Corporation. These particles were positively charged amidine latex and negatively charged sulfate latex spheres with two different diameters of 1.2 and 2.8 μm and a density of 1.055 g/cm^3. The surface charge densities σ of these particles provided by the manufacturer are shown in Table 1 with other particle properties. The sign and magnitude of their surface charge densities have been confirmed by the measurement of electrophoretic mobility[36),37)] and an analysis using the Gouy-Chapmann double layer model[14)] which expresses the electrical potential distribution from the isolated surface in a symmetrical electrolyte solution and Ohshima's equation of electrophoretic mobility taking into account of double layer relaxation.[38),39)] A KCl (JIS special grade, Wako Pure Chemical Industries) solution as an electrolyte was used to adjust electrolyte concentration. All solutions and suspensions were prepared using pure water (Elix, Millipore).

3.2. Turbulent hetero-coagulation experiments

Turbulent hetero-coagulation experiments were conducted in a cuvette with a square cross section (1 cm × 1 cm). The turbulent flow was generated by using a small magnetic stirrer (spinbar

Table 1 Properties of the particles used in present study: d particle diameter, σ surface charge density, N_A and N_S initial particle number concentration of amidine and sulfate latex in coagulation experiment.

Surface head-groups	d [μm]	σ [mC/m^2]	N_A or N_S [cm^{-3}]
Sulfate	2.8	-70	1.75×10^6
Amidine	2.8	+430	1.75×10^6
Sulfate	1.2	-96	2.11×10^7
Amidine	1.2	+206	2.11×10^7

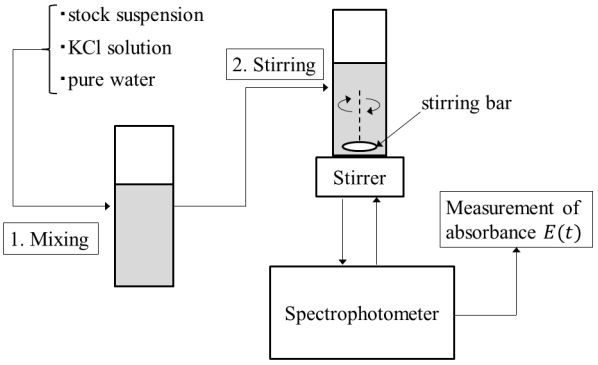

Fig. 2 The procedure of turbulent coagulation experiment in a turbulence generated by a small magnetic stirrer.

of 1.5 mm thickness and of 8 mm length). The schematic view of the experimental procedure is represented in Fig. 2. In this study, using combinations of the oppositely charged and equal-sized particles shown in Table 1, we focus on the effect of attractive double layer force on the hetero-coagulation of equal-sized particles.

The turbulent intensity in coagulation experiments was controlled by the rotational speed of the stirrer. We adopted two different speeds of 1491 (high shear) and 527 (low shear) rpm which were measured by a stroboscope. Since the turbulent intensity at each rotational speed was reflected in the rate of energy dissipation per unit mass ϵ_T and the rate of turbulent coagulation depends on ϵ_T, the ϵ_T was evaluated from the fast homo-coagulation rate constant of sulfate latex particles with a diameter of 2.8 μm. The fast homo-coagulation rate constant is the rate in the absence of electrical double layer force and is calculated by Eq. (1) with $\alpha_{T,SA} = \alpha_{T,0}$ given by

$$\alpha_{T,0} = \left(\frac{A_{\mathrm{H}}}{36\pi\mu R^3 \sqrt{\frac{4\epsilon_T}{15\pi\nu}}} \right)^{0.18} \tag{23}$$

where μ is the viscosity of the medium and the value of the Hamaker constant $A_{\mathrm{H}} = 10^{-21}$ J in the calculation is taken from the literature.[25] The results of the average local shear rate G_T were shown in Table 2.

In the hetero-coagulation experiments, as shown in Fig. 2, required volumes of positively and negatively charged latex suspensions, KCl solution and pure water were mixed in the cuvette and the total 2 mL of the mixture was stirred at high or low rotational speed. At predetermined intervals of stirring time, the absorbance of the mixed suspension $E(t)$ was measured by a spectrophotometer (Hitachi, U-1800) at wavelength 600 nm. The coagulation experiment was carried out as a function of particle size, turbulent intensity, and KCl concentration. From the temporal change of absorbance

Table 2 Evaluated turbulent intensity generated by a small stirrer: ω rotational speed of the small stirrer, ϵ_T the rate of energy dissipation per unit mass evaluated from the coagulation rate constant of 2.8 μm latex particles, $G_T = \sqrt{4\epsilon_T/(15\pi\nu)}$ the average local shear rate.

ω [rpm]	ϵ_T [m^2/s^3]	G_T [s^{-1}]
1491	1.21	329
527	0.199	133

$E(t)$ of the colloidal suspensions due to aggregation, the hetero-coagulation rate constant β_{SA} was determined. The initial number concentrations of amidine latex N_A and sulfate latex N_S were shown in Table 1. From the experimental curve of $E(t)$, the values of initial slope $dE/dt|_{t\to 0}$ and initial absorbance E_0 were obtained. These values were used to determine the absolute hetero-coagulation rate constant β_{SA} by neglecting the homo-coagulation between the same particles as follows.

$$\beta_{SA} = \frac{\frac{1}{E_0}\frac{dE}{dt}\Big|_{t\to 0}(C_S X_S + X_A C_A)}{N_0 X_S X_A (C_{SA} - C_S - C_A)} \tag{24}$$

where $N_0 = N_S + N_A$, $X_A = N_A/N_0$ and $X_S = N_S/N_0$ are the initial number concentration of the mixed suspension, the ratio of concentration of amidine and sulfate latex. C_A, C_S, and C_{SA} are extinction cross sections of amidine latex, sulfate latex, and the doublet of sulfate and amidine latex, respectively. The extinction cross sections were calculated using the T-matrix method.[26),30)] The pH values of suspensions were measured and were 5.2-6. In these pH values, the surface charges of sulfate and amidine latex particles are considered to be constant.[28),40)] All experiments were carried out at 20 °C.

4. RESULTS AND DISCUSSION

Figure 3 shows the typical plots for the temporal change of normalized absorbance E/E_0 of the suspension for the particles with a diameter of $2R = 1.2$ μm at different KCl concentrations in low shear flow corresponding to the rotational speed of the stirrer of 527 rpm. The figure indicates that the rate of decline of $E(t)$ increases with decreasing KCl concentration less than 10 mM, representing that the attractive electrical double layer force enhances the hetero-coagulation between the oppositely charged particles in lower KCl concentration. However, even at higher concentration above 10 mM, the rate also increases with increasing KCl concentration. The increase of the rate at high KCl concentration probably indicates simultaneous occurrences of homo-coagulation of sulfate-sulfate and amidine-amidine. That is, at such high KCl concentration, the repulsive double layer force between similarly charged particles becomes smaller than when it is at lower KCl concentration. The trends are more quantitatively shown by displaying the absolute hetero-coagulation rate constant as shown in Fig. 4.

Figure 4 shows the relationship between turbulent hetero-coagulation rate constant β_{SA} and KCl concentration for the oppositely charged particles. In Fig. 4, the circles and triangles are experimental values for the larger particles (2.8 μm) and smaller particles (1.2 μm), respectively. The closed and open symbols denote the results at high and low shear rates, respectively. The dashed and solid lines are theoretical values calculated by trajectory analysis with the Hamaker constant $A_{\mathrm{H}} = 10^{-20}$ J and $A_{\mathrm{H}} = 10^{-21}$ J. The thick and thin lines indicate the calculations for high and low shear rates, respectively. From the experimental values in Fig. 4, we see that the hetero-coagulation rate constant β_{SA} increases with decreasing KCl concentration and with increasing particle diameter

as well as turbulent intensity. The experimental rate constants around 1 and 10 mM KCl resulted in the minimum values at which the enhanced effect of the attractive double layer force on the hetero-coagulation is not significant due to the screening of electrical double layer. That is, the hetero-coagulation around 1 and 10 mM can be considered in the fast coagulation region where the attractive electrical double layer force is negligible in hetero-coagulation and the van der Waals force is dominant as physico-chemical forces controlling the rate of hetero-coagulation. To confirm this consideration for the results around 1 and 10 mM KCl, the relationship between the hetero-coagulation rate constant at 1 and 10 mM and $\epsilon_T^{0.41} R^{2.46}$ are shown in Fig. 5 following the Eqs. (1) and (23). The figure shows that the experimental values (symbols) around 1 and 10 mM are in good agreement with the calculation (line) obtained using trajectory analysis with $A_{\mathrm{H}} = 10^{-21}$ J without the double layer force; the hetero-coagulation rates are comparable to the fast rates in 1 and 10 mM. However, as mentioned above, at higher KCl concentration above 10 mM, the experimental rate constant apparently increased again with increasing KCl concentration. This apparent increase in hetero-coagulation rate is probably due to simultaneous occurence of homo-coagulation induced by decreased double layer repulsion, since such effect is neglected in Eq. (24).

In Fig. 6, we plotted the normalized turbulent hetero-coagulation rate constant by the fast hetero-coagulation rate constant $\beta_{SA,0}$ obtained at 10 mM, where the double layer attraction can be neglected, against KCl concentration in order to emphasize the influence of attractive electrical double layer force. Symbols, thick and thin lines are indicated by the same manner in Fig. 4. The solid and dashed lines are theoretical values calculated by trajectory analysis with the Hamaker constant $A_{\mathrm{H}} = 10^{-20}$ J for 1.2 μm and 2.8 μm, respectively. Fig. 6 shows that the normalized rate constant for the smaller particles (1.2 μm) depends more significantly on KCl concentration than that for the larger ones (2.8 μm). Similar trends are observed in theoretical prediction for the normalized rate constant in Fig. 6. These consistencies can be interpreted on the basis of Eq. (18) indicating that the maximum attractive double layer force between dissimilar surfaces is proportional to the square of smaller surface charge density σ_2^2 irrespective of larger one σ_1^2.[34] The smaller magnitude of charge density (-96 mC/m^2) between the particles with a diameter of 1.2 μm was larger than that (-70 mC/m^2) between the particles with a diameter of 2.8 μm as shown in Table 1. Therefore, we suggest that stronger double layer attraction in the case of 1.2 μm particles resulted in the enhanced hetero-coagulation rates both experimentally and theoretically.

In Figs. 4 and 6, with comparison between experimental (symbols) and theoretical (lines) values calculated by the trajectory analysis described above, we see that the theoretical prediction qualitatively agrees with experimental values. Especially, the dependence of theoretical values on KCl concentration in the presence of attractive double layer force is consistent with that of experiments.

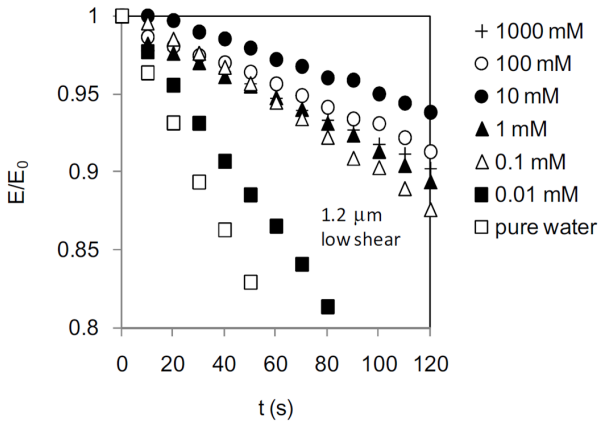

Fig. 3 The relationship between normalized absorbance E/E_0 and time t for the particles with a diameter of $2R = 1.2$ μm at different KCl concentrations in low shear flow.

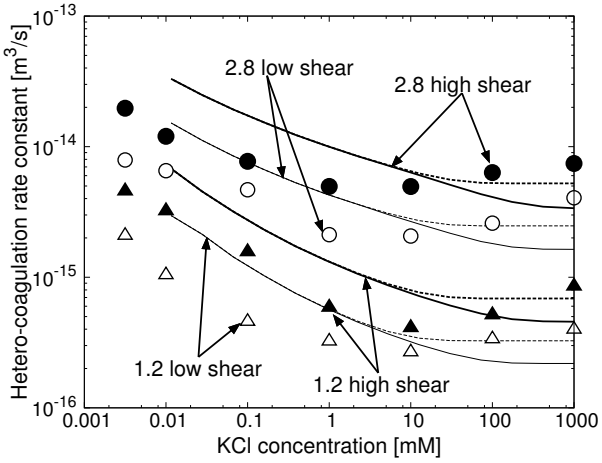

Fig. 4 Turbulent hetero-coagulation rate constant β_{SA} vs. KCl concentration for the oppositely charged particles: Symbols indicate experimental values. Dashed and solid lines are theoretical values calculated by trajectory analysis with the Hamaker constant $A_{\mathrm{H}} = 10^{-20}$ J and $A_{\mathrm{H}} = 10^{-21}$ J, respectively. Thick and thin lines are the calculated values for high and low shear rates, respectively.

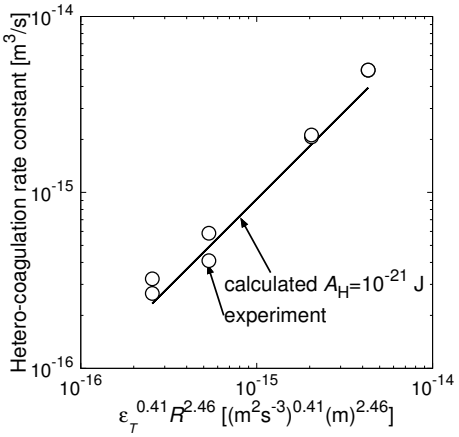

Fig. 5 Turbulent hetero-coagulation rate constant obtained at 1 and 10 mM KCl: The symbols indicate all the experimental values at 1 and 10 mM. The line is theoretical curve calculated by trajectory analysis with the Hamaker constant $A_{\mathrm{H}} = 10^{-21}$ J in the absence of electrical double layer force.

Therefore, we conclude that the trajectory analysis can capture the behavior of the shear-induced hetero-coagulation rate constant in a qualitative sense. By contrast, quantitative discrepancies between the theoretical and experimental values are clearly observed. These discrepancies are probably caused by the additional forces so-called non-DLVO forces[14),35)] or the inhomogeneous distribution of the surface charge[14)] and the inaccuracy of evaluation for the rate of energy dissipation per unit mass.

5. CONCLUSION

We measured the hetero-coagulation rates between oppositely charged particles in a turbulent flow generated by a stirrer. The experimental results show that the hetero-coagulation rate constant increases with decreasing KCl concentration and with increasing particle size as well as turbulent intensity. These trends qualitatively agree with the theoretical prediction based on the aggregation kinetics in a turbulence combined with a trajectory analysis including the attractive electrical dou-

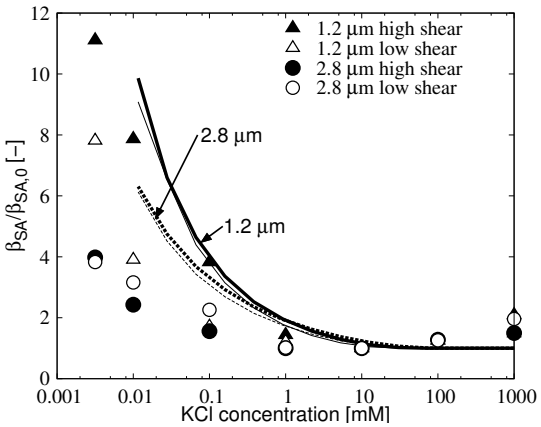

Fig. 6 Normalized turbulent hetero-coagulation rate constant $\beta_{SA}/\beta_{SA,0}$ vs. KCl concentration for the oppositely charged particles: Symbols are experimental values. Solid and dashed lines are theoretical values calculated by trajectory analysis with the Hamaker constant $A_{\mathrm{H}} = 10^{-20}$ J for 1.2 μm and 2.8 μm. Thick and thin lines indicate the calculation for high and low shear rates, respectively.

ble layer interactions. The facilitated coagulation rates in lower KCl concentrations are considered to be due to the increase of the magnitude of attractive double layer force accompanied by the development of electrical double layer.

ACKNOWLEDGMENT: We are grateful for the financial support from JSPS KAKENHI (15H04563) and Grant-in-Aid for JSPS Fellows (15J00805).

REFERENCES

1) Elimelech, M., Jia, X., Gregory, J., & Williams, R., *Particle Deposition & Aggregation: Measurement, Modelling and Simulation.*, (Butterworth-Heinemann, 1998).

2) Russel, W. B., Saville, D. A., & Schowalter, W. R., *Colloidal Dispersions.*, (Cambridge University Press., 1992).

3) Smoluchowski, M. V., "Versuch einer mathematischen Theorie der koagulationskinetik kolloider lsungen", *Z. Phys. Chem.*, Vol.92, (1917), pp.129-168.

4) Saffman, P., & Turner, J. S., "On the collision of drops in turbulent clouds", *J. Fluid Mech.*, Vol.1, (1956), pp.16-30.

5) Fuchs, V. N., "Über die stabilitt und aufladung der aerosole", *Zeitschrift für Physik*, Vol.89, (1934), pp.736-743.

6) Spielman, L. A., "Viscous interactions in Brownian coagulation", *J. Colloid and Interface Sci.*, Vol.33, (1970), pp.562-571.

7) Van de Ven, T. G. M., & Mason, S. G., The microrheology of colloidal dispersions VII. Orthokinetic doublet formation of spheres, *Colloid Polymer Sci.*, Vol.255, (1977), pp.468-479.

8) Zeichner, G. R., & Schowalter, W. R., "Use of trajectory analysis to study stability of colloidal dispersions in flow fields", *AlChE J.*, Vol.23, (1977), pp.243-254.

9) Honig, E. P., Roebersen, G. J., & Wiersema, P. H., "Effect of hydrodynamic interaction on the coagulation rate of hydrophobic colloids", *J. Colloid and Interface Sci.*, Vol.36, (1971), pp.97-109.

10) Derjaguin, B. V., & Landau, L., "The theory of stability of highly charged lyophobic sols and coalescence of highly charged particles in electrolyte solutions", *Acta Physicochem. U.S.S.R.*, Vol.14, (1941), pp.633-652.

11) Verwey, E. E. J. W., Overbeek, J. T. G., & Overbeek, J. T. J. T. G., *Theory of the Stability of Lyophobic Colloids.*, (DoverPublications. com, 1999).

12) Ottewill R. H., & Shaw, J, "Stability of monodisperse polystyrene latex dispersions of various sizes", *Discussions of the Faraday Society*, Vol.42, (1966), pp.154-163.

13) Schowalter, W. R., "Stability and coagulation of colloids in shear fields", *Annual Review of Fluid Mechanics*, Vol.16, (1984), pp.245-261.

14) Behrens, S. H., Christl, D. I., Emmerzael, R., Schurtenberger, P., & Borkovec, M., "Charging and aggregation properties of carboxyl latex particles: experiments versus DLVO theory", *Langmuir*, Vol.16, (2000), pp.2566-2575.

15) Arp, P. A., & Mason, S. G., "The kinetics of flowing dispersions VIII. doublets of rigid spheres (theoretical)", *J. Colloid and Interface Sci.*, Vol.61, (1977), pp.21-43.

16) Adler, P. M., "Interaction of unequal spheres I. hydrodynamic interaction: colloidal forces", *J. Colloid and Interface Sci.*, Vol.84, (1981), pp.461-473.

17) Wang, Q., "A study on shear coagulation and heterocoagulation", *J. Colloid and Interface Sci.*, Vol.150, (1992), pp.418-427.

18) Vanni, M., & Baldi, J. B., "Coagulation efficiency of colloidal particles in shear flow", *Avd. Colloid Interface Sci.*, Vol.97, (2002), pp.151-177.

19) Kobayashi, M., "Aggregation of unequal-sized and oppositely charged colloidal particles in a shear flow", *J. Applied Mechanics*, Japan Society of Civil Engineers, Vol.11, (2008), pp.517-523.

20) Kobayashi, M., "Kinetics of shear coagulation of oppositely charged particles: A trajectory analysis", *Theoretical and Applied Mechanics Japan*, Vol.56, (2008), pp.267-272.

21) Sugimoto, T., Kobayashi, M., & Adachi, Y., "Aggregation rate of charged colloidal particles in a shear flow: trajectory analysis using non-linear Poisson-Boltzmann solution", *J. Japan Society of Civil Engineers, Ser. A2 (Applied Mechanics)*, Vol.17 (2), (2014), pp.I_475-I_482.

22) Higashitani, K., Yamauchi, K., Matsuno, Y., & Hosokawa, G., "Turbulent coagulation of particles dispersed in a viscous fluid", *J. Chemical Engineering of Japan*, Vol.16, (1983), pp.299-304.

23) Adachi, Y., "Dynamic aspects of coagulation and flocculation", *Adv. Colloid and Interface Sci.*, Vol.56, (1995), pp.1-31.

24) Kobayashi, M., Maekita, T., Adachi, Y., & Sasaki, H., "Colloid stability and coagulation rate of polystyrene latex particles in a turbulent flow", *International J. Mineral and Processing*, Vol.73, (2004), pp.177-181.

25) Sato, D., Kobayashi, M., & Adachi, Y., "Capture efficiency and coagulation rate of polystyrene latex particles in a laminar shear flow: Effects of ionic strength and shear rate", *Colloids and Surfaces A*, Vol.266, (2005), pp.150-154.

26) Kobayashi, M. & Ishibashi, D., "Absolute rate of turbulent coagulation from turbidity measurement", *Colloid Polymer Sci.*, Vol.289, (2011), pp.831-836.

27) Sugimoto, T., Kobayashi, M. & Adachi, Y., "The effect of double layer repulsion on the rate of turbulent and Brownian aggregation: experimental consideration", *Colloids and Surfaces A*, Vol.443, (2014), pp.418-424.

28) Lin, W., Kobayashi, M., Skarba, M., Mu, C., Galletto, P. & Borkobec, M., "Heteroaggregation in binary mixtures of oppositely charged colloidal particles", *Langmuir*, Vol.22, (2006), pp.1038-1047.

29) Kobayashi, M., Nanaumi, H., & Muto, Y., "Initial deposition rate of latex particles in the packed bed of zirconia beads", *Colloids and Surfaces A*, Vol.347 (1), (2009), pp.2-7.

30) Sun, Z., Liu, J., & Xu, S., "Study on improving the turbidity measurement of the absolute coagulation rate constant", *Langmuir*, Vol.22, (2006), pp.4946-4951.

31) Batchelor, G. K., & Green, J. T., "The hydrodynamic interaction of two small freely-moving spheres in a linear flow field", *J. Fluid Mech.*, Vol.56, (1972), pp.375-400.

32) Ohshima, H., *Biophysical chemistry of biointerfaces*, (John Wiley and Sons, 2011).

33) Behrens, S. H., & Borkovec, M., "Electrostatic interaction of colloidal surfaces with variable charge", *J. Phys. Chem. B*, Vol.103, (1999), pp.2918-2928.

34) Ohshima, H., "Diffuse double layer interaction between two parallel plates with constant surface charge density in an electrolyte solution II. The interaction between dissimilar plates", *Colloid Polymer Sci.*, Vol.252, (1974), pp.257-267.

35) Israelachvili, J. N., *Intermolecular and Surface Forces Third Edition*, (Academic press, 2011).

36) Ottewill, R. H., & Shaw, J. N., "Electrophoretic studies on polystyrene latices", *J. Electroanalytical Chemistry and Interfacial Electrochemistry*, Vol.37, (1972), pp.133-142.

37) Kobayashi, M., "Electrophoretic mobility of latex spheres in the presence of divalent ions: experiments and modeling", *Colloid Polymer Sci.*, Vol.286, (2008), pp.935-940.

38) Ohshima, H., Healy, T. W., & White, L. R., "Approximate analytic expressions for the electrophoretic mobility of spherical colloidal particles and the conductivity of their dilute suspensions", *J. Chem Soc Faraday Trans 2*, Vol.79, (1983), pp.1613-1628.

39) Ohshima, H., "Approximate expression for the electrophoretic mobility of a spherical colloidal particle in a solution of general electrolytes", *Colloids and Surfaces A*, Vol.267, (2005), pp.50-55.

40) Kobayashi, M., Nitanai, M., Satta, N., & Adachi, Y., "Coagulation and charging of latex particles in the presence of imogolite", *Colloids and Surfaces A*, Vol.435, (2013), pp.139-146.